NOTATION

z, r, θ, axial, radial, and tangential coordinates; r_0, pipe radius, v_z, v_r, v_θ, time-averaged components of velocity; v'_z, v'_r, v'_θ, corresponding fluctuation components of velocity; ν, coefficient of kinematic viscosity; $N_{Re} = v_m r_0/\nu$, Reynolds number; v_m, mean-discharge velocity; L, pipe length, α, angle between the velocity vector and direction θ; $\nu_{ef} = \nu + \nu_t$; V_*, dynamic velocity.

LITERATURE CITED

1. B. E. Launder and D. B. Spalding, Mathematical Models of Turbulence, No. 4, Academic Press, London (1972).
2. O. L. Anderson, "A comparison of theory and experiment for incompressible turbulent swirling flows in axisymmetric ducts," AIAA Paper No. 72-43 (1972).
3. G. E. Sturov, in: Some Problems in Study and Industrial Application of the Eddy Effect [in Russian], Kuibyshev. Aviats. Inst., Kuibyshev (1974), p. 211.
4. D. G. Lilley and N. A. Chigier, "Nonisotropic turbulent flows from mean-value distributions," Int. J. Heat Mass Transfer, 14, 573 (1971).
5. B. E. Launder and D. B. Spalding, "Numerical computation of turbulent flows," Computer Methods Appl. Mech. Eng., 3, No. 2 (1974).
6. A. D. Gosman, V. M. Pan, A. K. Ranchel, D. B. Spalding, and M. Wolfstein, Numerical Methods of Analyzing the Flow of Viscous Fluid [Russian translation], Mir, Moscow (1972).
7. R. G. Backshall and F. Landis, "The boundary-layer velocity distribution in turbulent swirling pipe flows," ASME Paper No. 69-FE-14 (1969).
8. J. Laufer, "The structure of turbulence in fully developed pipe flow," Report No. 1174, NASA (1954).

EFFECT OF MASS FORCES ON PARTICLE MOTION IN A LAMINAR SUBLAYER OF TURBULENT FLOW IN RECTILINEAR CHANNELS WITH VARIOUS SPATIAL ORIENTATIONS

Yu. M. Grishin and A. A. Mosin

UDC 532.517

Based on solutions of the equations of motion, features of motion of a liquid particle are analyzed for a laminar sublayer of turbulent flow in channels with varying spatial orientations.

It is well known [1] that in solving the problem of particle precipitation at channel walls in a turbulent gas flow, the transverse particle motion is advisably considered separately in the flow bulk and in a narrow boundary layer with a large velocity gradient – the laminar sublayer. In the bulk flow the particle motion is uniquely determined by the action of turbulent flow pulsations on the particles [2] and obeys the laws of turbulent diffusion. In the boundary-layer region the effect of diffusion particle motion is weakened in comparison with systematic effects (due to fundamental forces). In this case it was shown [3] that particle precipitation at the channel walls is primarily determined by particle trajectories in the laminar sublayer. Despite the large number of papers devoted to calculating particle trajectories in the laminar sublayer (see, e.g., [4]), the problem of the effect of mass forces (weight forces), taking into account their interactions with forces generated in the fluid itself, on trajectories of particle motion in channels with varying spatial orientations has so far not been sufficiently investigated.

In this connection we consider the problem of motion of nondeformed particles of spherical shape in a laminar sublayer of an evolving turbulent flow moving in a rectilinear channel. We assume that the basic parameters of the boundary layer are independent of the channel orientation in space, do not vary along the channel (stable flow), and are determined by the well-known semiempirical relations [5]

Translated from Inzhenerno-Fizicheskii Zhurnal, Vol. 37, No. 2, pp. 260-268, August, 1979. Original article submitted October 2, 1978.

$$l/D = 25\mathrm{Re}_{\mathrm{av}}^{-7/8}, \quad W_0 = \frac{\nu}{D}\,\mathrm{Re}_{\mathrm{av}}^{7/8}, \quad W(y) = W_0\,\frac{y}{l}, \tag{1}$$

where $\mathrm{Re}_{\mathrm{av}} = U_{\mathrm{av}}D/\nu$.

We will further assume that the gas – particle system, i.e., the vapor – fluid drop, is a "dilute" system [6], i.e., $a/l \ll 1$, $a/R_a \ll 1$. In this case it can be assumed in first approximation that the velocity profile of the main flow is not deformed and that particles move without collisions [6]. Besides, it is assumed that $V_{\mathrm{rel}}/\nu \ll 1/a$.

Taking into account the approximations made, the equation of motion of an isolated particle under the action of Stokes, Magnus, Archimedes, and weight forces on it is [7]

$$\frac{d\mathbf{V}}{dt} = \mathbf{g}(1-\varkappa) - \frac{9}{2}\varkappa\frac{\nu}{a^2}(\mathbf{V}-\mathbf{W}) + \frac{3}{8}\varkappa\boldsymbol{\Omega}\times(\mathbf{V}-\mathbf{W}), \tag{2}$$

where $\boldsymbol{\Omega} = \mathrm{curl}\,\mathbf{W}$.

Introducing as characteristics the following quantities: the velocity W_0, the linear dimension l, and time $\tau^* = l/W_0$, we rewrite Eq. (2) in dimensionless form [further, beyond Eq. (3), the sign ~ is omitted over the dimensionless quantities]

$$\frac{d\tilde{\mathbf{V}}}{d\tilde{\tau}} = \alpha\mathbf{e} - \frac{\varkappa}{\mathrm{Re}}(\tilde{\mathbf{V}}-\tilde{\mathbf{W}}) - \frac{3}{8}\varkappa\frac{d\tilde{W}}{d\tilde{y}}\,\mathbf{k}\times(\tilde{\mathbf{V}}-\tilde{\mathbf{W}}), \tag{3}$$

where $\tilde{V} = V/W_0$; $\tilde{W} = W/W_0$; $\tilde{\tau} = t/\tau^*$; $\tilde{y} = y/l$; $\tilde{x} = x/l$; $\alpha = (1-\varkappa)/\mathrm{Fr}$; $\mathrm{Fr} = W_0^2/gl$; $\mathrm{Re} = \frac{2}{9}\frac{W_0 l}{\nu}\left(\frac{a}{l}\right)^2 = \frac{50}{9}\left(\frac{a}{l}\right)^2$.

The initial conditions to (3) are:

$$\tau = 0; \quad x = 0; \quad y = 1; \quad \frac{dx}{d\tau} = d; \quad \frac{dy}{d\tau} = -m. \tag{4}$$

The minus sign in front of m denotes that the variant is studied, in which the particle velocity at the initial moment of time is directed toward the wall of the channel.

Depending on the direction of the vector $\mathbf{e} = \mathbf{g}/g$, we distinguish the following two cases of channel orientation (Fig. 1): a) $\mathbf{e} = \pm\mathbf{e}_1$, a horizontal channel, with the plus sign at $\mathbf{e}_1$ corresponding to the precipitation problem at the upper channel wall, and the minus sign to the lower wall; b) $\mathbf{e} = \pm\mathbf{e}_2$, a vertical channel, with the plus sign corresponding to the precipitation problem for a downflow, and the minus sign for an upflow. The case $\alpha = 0$ corresponds to the precipitation problem at the channel wall in the absence of weight. For both cases mentioned the projections of Eq. (3) on the coordinate axes 0x and 0y form a system of two second-order linear differential equations in the two unknown particle coordinates x and y. The solution of this system with the initial conditions (4) is obvious, but is not given here due to its awkwardness.

We first clarify the features of particle motion in the channel for the case $\alpha = 0$, i.e., when there are no gravity forces. Depending on the value of $\mathrm{Re} \sim (a/l)^2$ we have the following two characteristic regions of particle motion in the flow:

1. $\mathrm{Re} < \mathrm{Re}_{\mathrm{cr}} = \varkappa/\left(\frac{m}{2} + \sqrt{\frac{m^2}{4} + \frac{3}{8}\varkappa\left(d - \frac{3}{8}\varkappa\right)}\right)$, the particle is not incident on the channel wall, moving in the sublayer parallel to the wall at a distance $y = y_\infty$ from it with flow velocity $V_x = W(y = y_\infty)$ (Fig. 2a), with

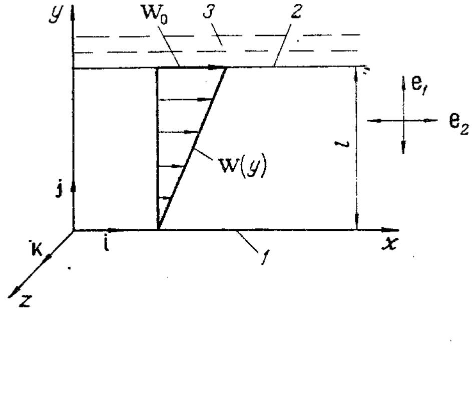

Fig. 1. Statement of the problem: 1) channel wall; 2) external boundary of laminar sublayer; 3) turbulent flow core.

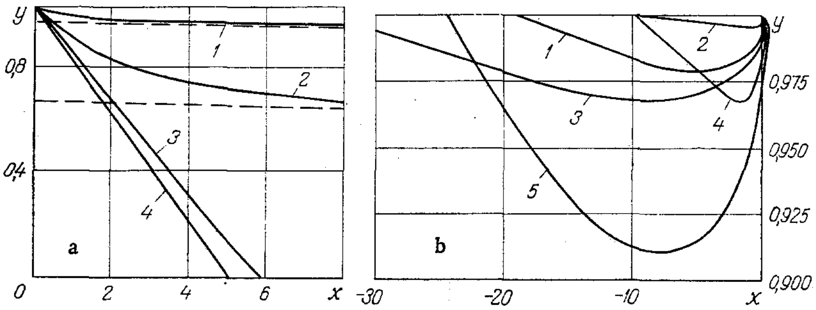

Fig. 2. Particle trajectories in the sublayer: a) horizontal channel [$\alpha = 0$; $\varkappa = 6 \cdot 10^{-4}$ (P = 1 atm); m = 0.2; d = 1]: 1) $\varkappa/\mathrm{Re} > 6 \cdot 10^{-1}$; 2) $6 \cdot 10^{-1}$; 3) $6 \cdot 10^{-2}$; 4) $6 \cdot 10^{-3}$; b) departure of particles from sublayer in a vertical channel with upflow motion [m = 0.2. For trajectories 1, 2, 3) $\alpha = -322$; d = 0.6; 4, 5) 32.2; 1]: 1) $\varkappa/\mathrm{Re} = 5.0$; 2) 50; 3) 0.5; 4) 5.0; 5) 0.5.

$$y_\infty = \frac{(\varkappa/\mathrm{Re})\,[(\varkappa/\mathrm{Re}) - m] + \frac{3}{8}\,\varkappa\left(\frac{3}{8}\,\varkappa - d\right)}{(\varkappa/\mathrm{Re})^2 + (3\varkappa/8)^2 - 3\varkappa/8};$$

2. $\mathrm{Re} > \mathrm{Re}_{cr}$, the particle settles at the channel wall during a flow time $\tau_c(m, d, \varkappa/\mathrm{Re})$ at some distance $x_c(m, d, \varkappa/\mathrm{Re})$ from the entrance to the sublayer (Fig. 2a).

The dependence of $\mathrm{Re}_{cr} = \frac{50}{9}\left(\frac{a}{l}\right)^2_{cr} = f(m, d, \varkappa)$ on pressure P is presented in Fig. 3 in coordinates of Re_{cr}, since $\varkappa = \varkappa(P)$ (the values of the vapor and fluid densities are taken from the saturation lines) for $P \in [1, P_{cr} = 226$ atm] and for various values of m and d = 1. It is seen from the figure, in particular, that with increasing pressure large-size particles [with $(a/l) > (a/l)_{cr}$] will settle at the channel walls under otherwise equal conditions, while for decreasing transverse component of particle velocity this tendency is enhanced. It must be noted, however, that with increasing pressure P the value of the transverse particle velocity (averaged over a distribution) at the entrance to the laminar sublayer is enhanced [2], and, consequently, the effect of decreasing precipitation intensity with increasing pressure is weakened. At first pressures ($\varkappa$ = const) the quantity y_∞ depends on Re and on the initial particle velocities m and d. With increasing Re (i.e., with increasing particle size a at l = const) the y_∞ value drops from 1 (Re = 0) to 0 at $\mathrm{Re} = \mathrm{Re}_{cr}$. For small values $m \ll (3/8)(\varkappa/\mathrm{Re})$ the quantity y_∞ is near 1, and is generally weakly dependent on any parameters. With increasing m, y_∞ decreases. An increase in the longitudinal component of the initial particle velocity leads formally to lower values of the coordinate y_∞, but for characteristic variation regions of Re, $\varkappa$, and m this effect is of little importance.

For $\mathrm{Re} > \mathrm{Re}_{cr}$ the particle settles on the channel wall during some time τ_c at a distance x_c from the entrance to the sublayer. For small pressure (close to atmospheric), i.e. for small $\varkappa$, in this case there is an "inertial" regime of particle movement in the sublayer, i.e., the particle practically moves in a rectilinear trajectory, retaining until collisions the values V_x and V_y of the velocity components near the initial d and m, respectively. In this case $\tau_c \simeq 1/m$ and $x_c \simeq d/m$. With increasing pressure and for Re near Re_{cr} the effect of forces at the side of the flow is enhanced, which is manifested in the bending of the particle trajectory, in the dependence of V_x and V_y on the particle position in the flow, etc. For small values of the initial particle velocity in the transverse

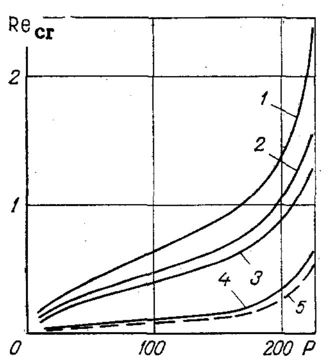

Fig. 3. Re_{cr} as a function of pressure P, atm [for the dependences 1, 2, 3) m = 0; 4, 5) 1]: 1) d = 0.6; 2) 1; 3) 1.4; 4) 0.6; 5) 1.4.

direction m < 0.2, the value of the longitudinal velocity component at the initial moment of time d has a significant effect on the quantity τ_c, while for increasing d, τ_c decreases. Thus, e.g., for $\varkappa = 0.344$ (P = 200 atm) and $a/l \cong 0.4$, τ_c decreases by an order of magnitude when d changes from 0.6 to 1.4. For larger values m > 0.6 the dependence $\tau_c(d)$ weakens. This effect is related to the significant influence of the Magnus force $F_M \sim (d-1)$ [see Eq. (3)]. Since the result of force action is determined by its moment $\sim F_M\tau_c$, and τ_c depends significantly on m and increases with decreasing m, for small m values the moment of F_M is large. For d > 1 the particle is accelerated by the Magnus force, and for d < 1 it is slowed down. We note that for otherwise equal conditions a decrease in Re leads to an increase in τ_c.

The particle equations of motion in a laminar sublayer with account of the action of weight forces were analyzed numerically by computer, with the quantity a/l acquiring five values in the range $1.4\cdot(10^{-1}$–$10^{-3})$, $\varkappa(P)$ acquired the values $6\cdot10^{-4}$ (P = 1 atm), $5.01\cdot10^{-2}$ (P = 70 atm), 0.344 (P = 200 atm), and each $\varkappa$ value corresponded to a triplet of α values (in absolute value):

$$\varkappa = 6\cdot10^{-4};\quad \alpha = 0.172;\ 1.72;\ 8.6;$$

$$\varkappa = 5.01\cdot10^{-2};\quad \alpha = 32.2;\ 3.22\cdot10^{2};\ 1.61\cdot10^{3};$$

$$\varkappa = 0.344;\quad \alpha = 2.33\cdot10^{2};\ 2.33\cdot10^{3};\ 1.16\cdot10^{4}.$$

For fixed $\varkappa$ (implying fixed pressure and saturation temperature) an increase in α implies a decrease in the average vapor flow velocities (Re_{cr}) in the tube.

We turn now to results of analyzing features of particle motion in a horizontal channel with account of gravity forces.

Precipitation at the Lower Channel Wall. For an initial particle velocity directed toward the wall it always settles at the channel wall. For fixed pressure in the channel the qualitative effect of the basic parameters is the following: with increasing $\mathrm{Re} \sim (a/l)^2$ (i.e., with increasing particle size) the particle stay period in the sublayer is shortened (Fig. 4); an increase in the main flow velocity (a decrease in α) leads to an increase in τ_c, which is particularly strongly manifested for small Re; the effect of the initial particle velocity along the flow d is unimportant for τ_c and is a finite particle velocity (for collisions with the wall) in the y direction V_{yc}, but under certain conditions ($\mathrm{Re} > \mathrm{Re}_{cr}$) there is a finite particle velocity in the x direction V_{xc}, which increases with d. The final value of the particle coordinate x_c is determined as a function of τ_c and d, while with increasing d, x_c increases monotonically. The effect of m and P is discussed below. Analysis of the results of numerical calculations and of analytic solutions of Eq. (3) shows that depending on the variation region of parameters, the particle can move in two different regimes.

1. The "Drift" Regime. The particle moves toward the channel wall practically in the whole portion (except the initial one) with a constant velocity in the transverse direction U^{h}_{dr},

$$U^{h}_{dr} = \frac{1}{\mathrm{Re\,Fr}}\,\frac{1-\varkappa}{\varkappa}\left\{\frac{9}{64} - \frac{3}{8\varkappa} + \frac{1}{\mathrm{Re}^2}\right\}^{-1}. \tag{5}$$

The longitudinal particle velocity follows the main flow velocity. As follows from Eq. (5), U^{h}_{dr} is independent of the initial particle velocity, but is a function $U_{dr} = U_{dr}(\mathrm{Re}, \mathrm{Fr}, P)$. Necessary conditions of presence of a drift regime are: $\beta = (\varkappa/\mathrm{Re})^2 + (3\varkappa/8)^2 - 3\varkappa/8 > 0$, $(\varkappa/\mathrm{Re}) > \alpha + m\sqrt{(3\varkappa/8)(1-3\varkappa/8)}$, and the larger the value of $\varkappa/\mathrm{Re}$ [corresponding to smaller $\mathrm{Re} \sim (a/l)^2$ at fixed P] the better they are satisfied, so that $(\varkappa/\mathrm{Re})^2 \gg (3\varkappa/8) - (3\varkappa/8)^2$, and, consequently, for most interesting cases Eq. (5) can be represented in the form ($\varkappa \ll 1$)

$$U^{h}_{dr} \simeq \frac{\mathrm{Re}}{\mathrm{Fr}\,\varkappa} = \frac{g\sqrt[8]{D}}{5}\,\frac{a^2}{U_{av}^{7/8}}\,F_1(P), \tag{6}$$

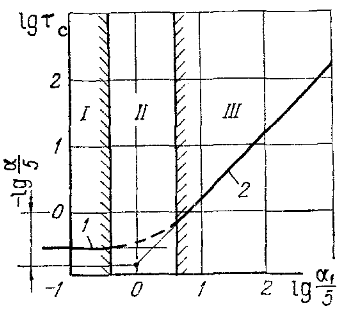

Fig. 4. Dependence of τ_c on $\alpha_1 = \varkappa/\mathrm{Re}$ for precipitation at lower wall of horizontal channel [the continuous line is an approximate calculation by Eqs. (5)-(7); the dotted line is the calculation by Eq. (3)]: 1) $\tau_c = \sqrt{2(1-\chi)/\alpha}$; 2) $1/U^{h}_{dr}$; I) "free-fall" region; II) transition region; III) "drift."

where $F_1(P) = 1/[\varkappa(P)\nu^{9/8}(P)]$. The calculated $F_1(P)$ for the vapor – water system at the saturation line is a decreasing monotonic function for increasing pressure P. Consequently, with increasing P the drift velocity U^h_{dr} decreases $[U^h_{dr}(P = 1)/U^h_{dr}(P = 226\ \text{atm}) \simeq 6]$. The effect of the remaining parameters on U^h_{dr} is easily seen from Eq. (6). We only note the quite strong dependence of U^h_{dr} on the particle size $U^h_{dr} \sim a^2$ and the very weak effect of the steam pipe diameter $U^h_{dr} \sim \sqrt[8]{D}$.

2. The "free-fall" regime is characterized by a strong influence on the trajectory of particle motion due to gravity with very insignificant effect of flow forces. This regime is realized for sufficiently large particle sizes a (in comparison with the sublayer width l). A necessary condition for the existence of this regime is $\beta < 0$. The particle velocity in the flow and the time up to collisions with the channel wall are quite accurately described by Eq. (3), in which, considering only the first term in the right-hand side of αe:

$$V_x = d, \quad V_y = -m - \alpha\tau,$$

$$\tau_c \simeq -\frac{m}{\alpha} + \sqrt{\frac{m^2}{\alpha^2} + \frac{2}{\alpha}}, \quad V_{yc}/m = (1 + 2\alpha/m^2)^{1/2}. \tag{7}$$

Comparison of results of calculations by Eq. (7) with exact calculations by Eq. (3) is satisfactory. The effect of separate system parameters in this motion regime is seen from Eq. (7). Here we note the fact that for sufficiently large-scale particles, for which the existence condition of this regime is realized, the particle size and pressure in the system have small effect on the trajectory and on other parameters.

Figure 4 shows comparison of dependences of τ_c on $\varkappa/\text{Re}$ for P = 70 atm, constructed by Eq. (3) and by means of the approximate relations (5), (7). Satisfactory agreement of the constructed curves in the regions of parameter values $\varkappa/\text{Re}$, corresponding to the regimes of "free-fall" and "drift" of particle motion, is easily seen. A transition region is found between these regions, in which the particle motion cannot be described by any of the suggested approximations, and it is necessary to use the rigorous solution of Eq. (3).

Precipitation at the Channel Top Wall. One of the main features of liquid particle precipitation in a vapor flow in thermodynamic equilibrium at the channel top wall is the difficulty in its advance toward the wall due to gravity and drag forces. From the whole variation region of basic parameters, for which numerical analysis of solutions of Eq. (3) was performed, particle precipitation at the channel wall occurs only for $\alpha = 0.172$ and $\varkappa = 6 \cdot 10^{-4}$ (P = 1 atm), m > 0.6 for certain values of $\varkappa/\text{Re}$, smaller than some critical value $(\varkappa/\text{Re})_{cr}$ which is a function of $\varkappa$, α, m. If the system parameters are such that $(\varkappa/\text{Re}) > (\varkappa/\text{Re})_{cr}$, the particle is not incident at the channel wall and leaves the sublayer at some time $\tau_c(m, \varkappa/\text{Re})$, while τ_c decreases with decreasing m and increasing $\varkappa/\text{Re}$, i.e., the particle stay period in the sublayer is shortened with decreasing initial particle velocity in the transverse direction, with increasing pressure in the system, and decreasing particle size. One cannot establish an analytic dependence of $(\varkappa/\text{Re})_{cr}$ on the basic system parameters starting from the solution of Eq. (3), since it is necessary to obtain the solution of a corresponding transcendental equation. Using results of numerical calculations, one notes two limiting regions of basic parameter changes, for which the particle certainly reaches the channel wall and leaves the sublayer. The first case occurs for $\beta \leq 0$, when $\alpha \leq m^2/2$, while the second is realized for $\beta > 0$ and

$$\alpha \geqslant \left\{\beta^2 + m\,\frac{\varkappa^3}{\text{Re}}\left[\frac{1}{\text{Re}^2} + \left(\frac{3}{8}\right)^2\right] - \frac{3\varkappa m}{8}\right\} \Big/ \beta.$$

Taking into account the remarks made above, we note the substantial nonuniformity of particle precipitation intensity along the channel perimeter in a horizontally placed channel, which may be the reason for an anisotropic distribution of a liquid-phase film at the channel wall in the presence of a dispersed-ring flow region of the vapor – liquid system in it.

We now consider particle motion in a vertical channel with account of gravity forces on the system, while we distinguish between down- and upflow.

Particle Precipitation for Downflow. The given case is characterized as follows: for the whole variation region of basic parameters considered the particle settles at the channel wall, which is related to Magnus force action, which is transversally directed due to the accelerating action in the x direction by the particle gravity force, directed toward the channel wall (this leads to the fact that the particle moves faster than the vapor flow for d > 1 during the whole time, and for d < 1 after some initial time interval). We mention some basic features of precipitation. For fixed pressure in the system a decrease in Re $\sim (a/l)^2$ leads to an increase in the particle stay time in the flow τ_c, an increase in the parameter α under otherwise equal conditions has a very small effect on τ_c for large values of $\varkappa/\text{Re}$ larger than some critical value, and stronger (toward shortening τ_c) for small $\varkappa/\text{Re}$. For fixed Re an increase in pressure P and related parameters (temperature, vapor viscosity, etc.) leads to shortening of the particle stay time in the sublayer, while this dependence is very strong for small values of $\varkappa/\mathrm{Re}$. It must be noted that with increasing pressure the particle velocity is enhanced at large Re and significantly exceeds the main flow velocity, which, according to Eq. (3), leads to a sharp increase in the Magnus force directed toward the channel wall. The Stokes drag force has no practical effect. Since the expression for the Stokes force, used in Eq. (3), is valid for the case of small relative flow and particle velocities, $V_{rel\,max}/\nu \ll 1/a$ [or $V_{rel\,max} \ll 1/(5\sqrt{\mathrm{Re}})$]. In the cases mentioned this condition is violated and the results, rigorously speaking, are incorrect for quantitative estimates of τ_c and other quantities.

Analysis of the results obtained shows that the whole set of possible particle motions in the downflow sublayer can be developed for two characteristic motion regimes. The realization criterion of one or another regime is the magnitude of the parameter $\varkappa/\mathrm{Re}$. If $(\varkappa/\mathrm{Re}) > (\varkappa/\mathrm{Re})_{cr}$, after some time interval the particle starts moving toward the channel wall with a constant velocity U^0_{dr} in the transverse direction

$$U^0_{dr} = \frac{3}{8}\frac{\varkappa\alpha}{\beta}.$$

The particle velocity U^0_{dr} and the precipitation time τ_c are practically independent of the initial values of the particle velocity.

For $(\varkappa/\mathrm{Re}) \ll (\varkappa/\mathrm{Re})_{cr}$ we have a regime of "inertia" precipitation, when the value of the initial particle velocity practically does not change.

As shown by analysis, in first approximation the quantity $(\varkappa/\mathrm{Re})_{cr}$ coincides with the value of $(\varkappa/\mathrm{Re})_{cr}$ for the case of absence of gravity, so that for $\mathrm{Re} < \mathrm{Re}_{cr}$ we have the "drift" regime of particle motion. Taking into account for most cases $\beta \simeq (\varkappa/\mathrm{Re})^2$, as well as using Eqs. (1), (3), we write for U^0_{dr}

$$U^0_{dr} = \frac{3}{8\,(25)^2}\,\frac{a^4}{\sqrt[8]{D}}\,U^{7/8}_{av}\,F_2(P), \tag{8}$$

where $F_2(P) = 1/[\varkappa(P)\nu^{23/8}(P)]$.

The effect of separate parameters of the system on the particle velocity in the transverse direction and on $\tau_c = 1/U^0_{dr}$ is seen from Eq. (8). The function $F_2(P)$ increases with pressure, so that with increasing pressure U^0_{dr} increases, τ_c is shortened, and, consequently, the precipitation conditions improve. We note the important effect of particle size and of the main flow velocity on the precipitation rate.

For $(\varkappa/\mathrm{Re}) < (\varkappa/\mathrm{Re})_{cr}$ the basic features of the case $\alpha = 0$ are retained.

Particle Precipitation for Upflow. For this case of motion the result of acting forces is such that the particle can reach the channel wall only under certain conditions. As in the previous cases, the criterion separating these two variants is the quantity Re_{cr}. If $\mathrm{Re} < \mathrm{Re}_{cr}$ the particle leaves the sublayer under the action of Magnus forces. If $\mathrm{Re} > \mathrm{Re}_{cr}$ the particle reaches the channel walls.

The nature of particle emergence from the sublayer at $\mathrm{Re} < \mathrm{Re}_{cr}$ can differ. This difference consists of the following (Fig. 2b): either the particle, moving with almost constant velocity in the x direction in the flow, drifts with a constant velocity in the transverse direction to the exit from the sublayer, or at some point it turns around and moves toward the flow under the action of gravity forces, leaving the sublayer at a point found at some distance above the flow, away from the particle exit in the sublayer.

When the particle settles at the channel wall ($\mathrm{Re} > \mathrm{Re}_{cr}$), its precipitation time τ_c depends strongly on the magnitude of the initial particle velocity in the transverse direction and decreases with increase of the latter. The value of the initial particle velocity in the longitudinal direction has a weak effect on τ_c in the parameter region considered. The quantity α affects τ_c insignificantly, but considerably affects the coordinate of the particle precipitation point x_c. Thus, e.g., for $\alpha = -1.72$ (P = 1 atm) $x_c < 0$, while for $\alpha = -0.172$ (P = 1 atm) $x_c > 0$.

NOTATION

x, y, z, Cartesian coordinates; **e**, **i**, **j**, **k**, unit vectors; l, layer thickness; W_0, flow velocity at the upper boundary of the laminar sublayer; W(y), flow velocity distribution over the sublayer thickness; D, equivalent channel diameter; ν, kinematic vapor viscosity; U_{av}, average flow rate of the turbulent flow; Re, Reynolds numbers; a, particle radius; R_a, interparticle distance; V_{rel}, particle velocity relative to the gas; **V**, particle velocity; $\varkappa$, vapor to liquid particle density ratio; **g**, gravity force vector; t and τ^*, flow and characteristic times; m and d, dimensionless longitudinal and transverse particle velocities; P, pressure; F_M, Magnus force; Fr, Froude number; U_{dr}, particle drift velocity; α and β, dimensionless parameters.

LITERATURE CITED

1. P. L. Kirillov and I. P. Smogalev, Preprint FÉI-191 (1969).
2. P. L. Kirillov, I. P. Smogalev, and M. Ya. Suvorov, Teplofiz. Vys. Temp., 14, No. 1 (1976).
3. N. Kondic, Teploperedacha, 93, No. 3 (1970).
4. L. A. Ignat'evskaya, Candidate's Dissertation, Moscow Power Institute (1971).
5. V. M. Case, Convective Heat and Mass Transfer [Russian translation], Énergiya, Moscow (1972).
6. J. Happel and H. Brenner, Low Reynolds Number Hydrodynamics, Prentice-Hall, New Jersey (1965).
7. S. J. Rubinov and J. B. Keller, J. Fluid Mech., 11, 3 (1961).

NONSTEADY HOT-FILAMENT METHOD USING AN RC OSCILLATOR TO INVESTIGATE HEAT EXCHANGE IN RAREFIED GASES

Yu. G. Semenov, B. A. Kalinin,
S. F. Borisov, and P. E. Suetin

UDC 536.2.083

A device which realizes the nonsteady hot-filament method using an RC oscillator is discussed, along with the results of its testing in the measurement of the thermal conductivity of the gases Ar, N_2, and CO_2 and their mixtures under standard conditions.

The experimental investigation of heat exchange in rarefied gases in the presence of solid surfaces has acquired ever greater importance in recent years. The complex physicochemical processes taking place at the gas – solid boundary have a considerable effect on processes of heat transfer in gaseous media, requiring the introduction into heat-conduction theory of the concepts of a temperature jump and of coefficients of energy accommodation [1]. This imposes higher demands on the experimental technique also. The effort to satisfy these demands led us to the creation of a device based on the nonsteady hot-filament method using an RC oscillator as the recorder of the filament temperature.

A whole series of methods exist which permit one to investigate the thermophysical properties of a gaseous medium with a high degree of accuracy. The steady-state research methods have obtained the greatest development. Devices based on these methods possess a high measurement accuracy, but they have a number of fundamental drawbacks reducing the value and reliability of the results obtained. First of all one must note the presence of a constant temperature drop in the investigated gases, which leads to such undesirable phenomena as convection and thermodiffusion. The large value of this drop, reaching tens of degrees, hinders the one-to-one correlation between the results obtained and the temperature of the investigated gas. The time consumed in performing the measurements is long.

Devices based on nonsteady methods have not obtained wide application because of their low accuracy, which is due mainly to the difficulty in the recording of a rapidly varying temperature. All the same, nonsteady devices allow one to avoid the indicated defects of steady-state devices, and they considerably simplify and speed up the measurement process.

To increase the accuracy of nonsteady devices we used a high-frequency RC oscillator as the temperature recorder. A circuit diagram of the device is shown in Fig. 1. The electronic circuit built on the transistors T_1 and T_2 together with the detector D form an RC oscillator whose negative feedback circuit is frequency-setting and is built in the form of a 2T bridge.

S. M. Kirov Ural Polytechnic Institute, Sverdlovsk. Translated from Inzhenerno-Fizicheskii Zhurnal, Vol. 37, No. 2, pp. 269-272, August, 1979. Original article submitted October 2, 1978.